INSTITUT DE FRANCE
Académie des sciences

Comptes Rendus

Physique

H. Mhiri, A. Jemni and H. Sammouda

Thermal behavior of Composite Material (nanoPCM/aluminum foam) used for thermal energy storage (TES) applications

Volume 21, issue 3 (2020), p. 233-252

Published online: 12 June 2020
Issue date: 19 November 2020

https://doi.org/10.5802/crphys.2

Les Comptes Rendus. Physique *sont membres du*
Centre Mersenne pour l'édition scientifique ouverte
www.centre-mersenne.org
e-ISSN : 1878-1535

Comptes Rendus
Physique
2020, 21, nº 3, p. 233-252
https://doi.org/10.5802/crphys.2

Research Article / *Article de recherche*

Thermal behavior of Composite Material (nanoPCM/aluminum foam) used for thermal energy storage (TES) applications

Comportement thermique d'un Matériau Composite (nano-MCP/mousse d'aluminium) utilisé pour des applications de stockage d'énergie thermique (TES)

H. Mhiri [*, a], **A. Jemni** [a] **and H. Sammouda** [a]

[a] University of Sousse- Laboratory of Energy & Materials (LabEM-LR11ES34), Rue Lamine Abbassi, 4011 Hammam Sousse, Tunisia

E-mail: mhirihiba@yahoo.fr (H. Mhiri)

Abstract. Thermal energy storage systems (TESS) using phase change materials (PCM) have attracted interest in various fields of science and technology. However, the interest of these systems is limited by the relatively low thermal conductivity of PCMs and their leakage in the melted state. To overcome these drawbacks, the present paper suggests a new alternative for the enhancement of the PCMs by incorporating highly conductive materials, such as metal foam and/or nanoparticles. A Direct Numerical Simulation (DNS) was carried out to investigate the melting process of paraffin wax as PCM enhanced with alumina nanoparticles (i.e. nanoPCM) embedded in aluminum foam under constant temperature. A three-dimensional (3D) foam regular structure was designed. The effects of aluminum foam porosity and nanoparticles' volume fraction on the thermal behavior of composite PCMs were investigated. The two-temperature model based on the assumption of local thermal non equilibrium was applied due to the great difference of thermal conductivity between nanoPCM and aluminum foam.

The results showed that both aluminum foam and alumina nanoparticles (Al_2O_3) significantly accelerate the melting process. Furthermore, the effective thermal conductivity of composite PCM (nanoPCM/aluminum foam) drastically increased. The DNS results showed important temperature difference between PCM and metallic ligament, assuring the viability of local thermal non-equilibrium.

Résumé. Les systèmes de stockage de l'énergie thermique (TESS) utilisant des matériaux à changement de phase (MCP) ont suscité l'intérêt dans divers domaines de la science et de la technologie. Cependant, l'intérêt de ces systèmes est limité par la conductivité thermique relativement faible des MCP et leur fuite à l'état fondu. Pour surmonter ces inconvénients, le présent document propose une nouvelle alternative pour l'amélioration des MCP en incorporant des matériaux hautement conducteurs, tels que mousse métallique et/ou nanoparticules. Une simulation numérique directe (DNS) a été réalisée pour étudier le processus de

* Corresponding author.

fusion de la cire de paraffine comme MCP amélioré par des nanoparticules d'alumine (c-à-d un nano-MCP) incorporées dans de la mousse d'aluminium à température constante. Une structure tridimensionnelle (3D) régulière de la mousse a été conçue. Les effets de la porosité de la mousse d'aluminium et de la fraction volumique des nanoparticules sur le comportement thermique des MCP composites ont été étudiés. Le modèle à deux températures basé sur l'hypothèse d'un non-équilibre thermique local a été appliqué en raison de la grande différence de conductivité thermique entre le nano-MCP et la mousse d'aluminium.

Les résultats ont montré que la mousse d'aluminium et les nanoparticules d'alumine (Al_2O_3) accélèrent toutes deux de manière significative le processus de fusion. En outre, la conductivité thermique effective du MCP composite (nano-MCP/mousse d'aluminium) a augmenté de manière drastique. Les résultats de la DNS ont montré une différence de température importante entre le MCP et le ligament métallique, assurant la viabilité du non-équilibre thermique local.

Keywords. Alumina nanoparticles, Aluminum foam, Phase change material, Thermal energy storage, Direct numerical simulation.

Mots-clés. Nanoparticules d'alumine, Mousse d'aluminium, Matériau à changement de phase, Stockage d'énergie thermique, Simulation numérique directe.

Manuscript received 13th August 2019, revised 23rd September 2019, accepted 3rd March 2020.

Nomenclature

C_p	Heat Capacity ($J{\cdot}kg^{-1}{\cdot}K^{-1}$)
K	Thermal conductivity ($W{\cdot}m^{-1}{\cdot}K^{-1}$)
L	Latent heat (J/kg)
T	Temperature (K)
T_m	Melting Temperature of PCM (K)
$\vec{u}$	Velocity (m/s)

Greek symbols

ρ	Density ($kg{\cdot}m^{-3}$)
β	Thermal expansion coefficient (1/K)
μ	Viscosity ($N{\cdot}s/m^2$)

Subscripts

Al_2O_3	Alumina nanoparticle
liquid	Liquid PCM
nanoPCM	PCM nanocomposite
nf	NanoPCM
PCM	Phase change material
s	Metal foam
solid	Solid PCM

1. Introduction

Thermal energy storage systems (TESS) are considered as an especially efficient way to minimize the mismatch between demand and supply of energy. Phase Change Materials (PCM) present one of the promising storage techniques due to their ability for charging and discharging heat at a constant temperature during the phase change process [1, 2]. In fact PCMs are classified into three types: organic, non-organic and eutectics [3].

Organic PCMs keep high density energy storage. They are accessible in a large temperature range and are compatible with different materials. Paraffin wax, fatty acids and carbohydrates are the most frequently used PCMs in this category [4].

Non-organic PCMs have high heat of fusion. They are non-flammable and could be obtainable at low costs. Nevertheless, their main drawbacks are their supercooling problem during the phase change process [5]. Hydrated salts are the foremost habitually used PCM for thermal energy storage in this group.

Eutectic PCMs are mixtures of two or more compounds. They have higher densities than organic materials. The main criterion to select a PCM for a specific application is its phase change temperature. Additionally, different factors should be taken into consideration for an appropriate choice. Among these factors are physical properties, non-toxicity, large latent heat of fusion, chemical stability and non-erosiveness.

Organic PCMs are considered as vital materials which have a high potential for applications in solar energy storage, greenhouse construction, recuperation of heat from electronic devices etc. In spite of their fascinating properties, organic PCMs have some drawbacks such as (i) the low thermal conductivity which reduces the rate of heat storage and energy conversion and, therefore, (ii) the leakage of materials during the solid-liquid phase change process. Many methods have been suggested to enhance the electrical and thermal conductivity of pure paraffin, such as inserting fins [6], metal foam [7], dispersing conductive particles within PCMs [8] and microencapsulation of PCMs [9]. With the development of nanotechnology, combining these pure PCMs with high conductive nanoparticles could be crucial to overcome these problems [10]. Thanks to their excellent properties [11–16], nanoparticles, such as carbon nanotubes, carbon Nanofibers, metallic nanoparticles, graphene flakes, etc [17–21] have gained considerable attention in many emerging applications like antistatic coatings, organic light emitting diodes, sensors, flexible microelectronics, and touch screens. A lot of numerical and experimental research has been carried out to improve the low thermal conductivity of PCMs by adding nanoparticles [22–27]. Kant *et al.* [28] examined the influence of inserting graphene nanoparticles (GNP) with different concentrations in various PCMs ($CaCl_26H_2O$, Capric Acid and paraffin). They numerically investigated the fusion of these composite materials inside a square cavity heated from one side. They revealed that inserting GNP improves the effective thermal properties of the PCMs and ameliorates the phase change rate. Arasu *et al.* [29] numerically investigated the melting of nanocomposite (PCM/Al_2O_3 nanoparticles) with different weight ratios which was heated from two different arrangements. The study revealed that the melting rate decreases with the increase of the concentration of alumina (Al_2O_3). The simulation showed that the accumulation of alumina in paraffin wax enhances the thermal properties which are required for an efficient use of TESS. Additionally, the nanoPCMs can be used to cool down electronic devices. Moreover, such nanoPCMs have good insulation properties such as a high electrical resistivity and low relative permittivity. Wang *et al.* [30] prepared paraffin/nano-SiO_2 composites by natural infiltration method as innovative insulation materials applied to electronic thermal protection. Thermo gravimetric analysis (TGA), scanning electron micrography (SEM), hot disk analysis, differential scanning calorimetry (DSC) and thermal protection performance tests were carried out to examine the thermal properties, morphology and thermal protection performance of composites. Experimental results showed that the incorporation of about 75 wt% of nanoSiO_2 can mainly enhance the thermal properties of the nanocomposite. These excellent properties make the paraffin-nano-SiO_2 composite promising for use in the field of electronic thermal protection. Shirazi *et al.* [31] investigated the feasibility of using PCM nanocomposites for suitable heat management of a Li-ion battery package. The heat generation was modeled using 3D heat transfer model with different nanocomposite structures created by adding carbon nanotubes, graphene, and fullerene throughout the battery charging/discharging cycles. These results revealed a decrease in temperature variation by embedding the batteries within a paraffin nanocomposite and an enhancement of the effective thermal conductivity.

On the other hand, metal foam, as a novel material, has recently attracted considerable at-

tention because of its good mechanical and thermo-physical properties. Its interesting advantage includes low bulk density due to its high porosity, high specific strength and stiffness, and especially the high thermal conductivity of its continuous skeleton structure [32, 33]. Recently, a lot of studies have been carried out on the heat transfer of PCMs with metal foam. Xiao [34] prepared copper foam and nickel foam with different geometric parameters impregnated with paraffin through vacuum assistance. Results showed that the thermal conductivities of composite material have been considerably improved as compared to that of pure paraffin, e.g. the thermal conductivity of the composite paraffin/nickel foam is approximately three times higher than that of pure paraffin, while the thermal conductivity of the composite paraffin/copper foam is approximately 15 times higher than that of pure paraffin. Li *et al.* [35] discussed the possibility to enhance the latent heat thermal energy storage by microencapsulated phase change material (MEPCMs). They analyzed the thermal behavior of the composite by comparing it with two control groups, i.e. pristine PCM and PCM/foam modules. In particular, the thermal non equilibrium effect between foam strut and the microencapsulated phase change materials was quantitatively investigated. Chen *et al.* [36] developed a thermal lattice Boltzmann model with doubled populations to simulate the melting process of PCM in metal foams at the pore level. The numerical results showed that heat conduction in metal foam plays an important role in the melting of PCM while convection flow exerts little influence, which indicates that the existence of metal foam might cause the increase of flow resistance in the domain. Recently, Tao *et al.* [37] have studied the latent heat storage performance of copper foam/paraffin (CPCM) based on Lattice Boltzmann Method. They assumed the homogeneity of the metal foam and the uniformity of the pore diameter. They analyzed the effects of metal foam geometric parameters on heat conduction and natural convection heat transfer performance, PCM melting rate, thermal energy storage capacity and thermal energy storage density. Li *et al.* [38] developed a two-dimensional numerical model considering the non-Darcy effect, local natural convection to analyze the phase change heat transfer of PCMs in homogenous metal foams. They predicted the velocity, the temperature fields, and the evolution of the solid-liquid interface location at various times. The results indicated that the melting heat transfer is enhanced by the high thermal conductivity foam matrix, although its existence suppresses the local natural convection.

The improvement of phase change performance with the use of nanoparticles and porous medium has motivated researchers to examine the influence of adding both nanoparticles and metal foams concurrently in the phase change processes. The primary work that considered the melting of a nanoPCMs impregnated in a porous medium was achieved by Hossain *et al.* [39]. The authors examined the melting process of nanoPCM embedded in a porous medium. Aluminum foam was selected as the porous medium and the mixture Cyclohexane and CuO with different volume fractions was used as the nanoPCM. 2D numerical study investigated the thermal behavior of the nanoPCM inside metal foam. The results showed that the melting rate of PCM with both the porous medium and the nanoPCMs is faster than that of PCM with nanoparticles or porous medium. To the best of our knowledge, the research about melting nanoPCM inside porous media has rarely been studied in the literature. In the present work, a numerical study is proposed to predict and investigate the thermal characteristics of composite nanoPCM. We have modeled novel energy conversion and storage material by combining paraffin wax as a phase change material and alumina nanoparticles (Al_2O_3) as a thermal conductivity enhancer in open cell aluminum foam as a base structure. Current research proposes a direct numerical simulation (DNS) for both numerical modeling and scale analysis. Our numerical findings may improve our understanding of phase change processes for the nanoPCM inside metal foam. Hence, metal foam with regular periodic cell structure is designed. Taking into account the non-thermal balance between metal foam and nanoPCM, this paper presents an investigation of the thermal field of this composite material, the effects of heat conduction through metal foam structures, natural convection

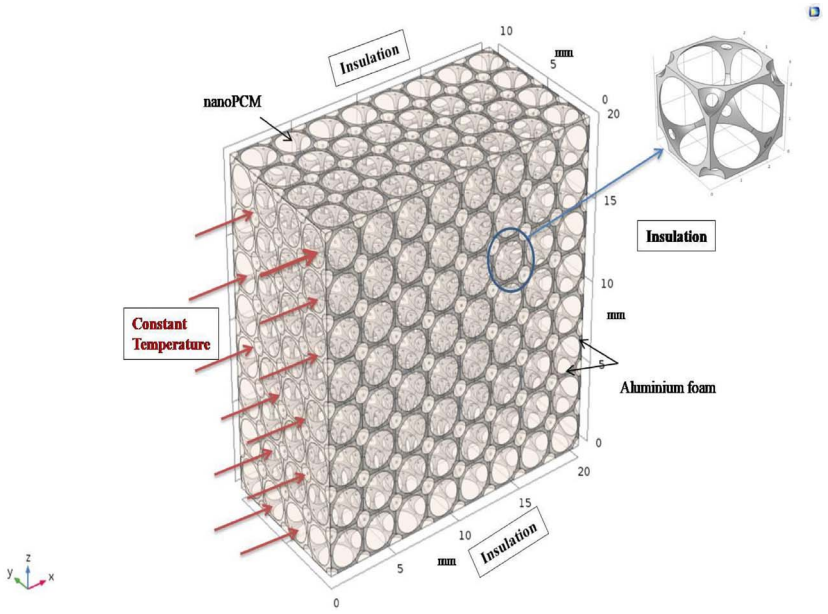

Figure 1. Reconstruction of open cell aluminum foam with regular cellular morphology.

of liquid nanoPCM, and the detailed parameters such as the porosity of metal foam and volume fractions of nanoparticles.

2. Physical model

The thermal behavior of the composite PCMs (aluminum foam/paraffin/Al_2O_3) with different parameters was investigated under unsteady state. The mixture Paraffin wax/Al_2O_3 nanoparticles were impregnated in the pore space of aluminum foam as nanoPCM.

The Direct numerical simulation (DNS) requires the reconstruction of the open-cell foams geometry. In the present study, the cellular morphology of the aluminum foam was modeled with a regular porous structure, which is easy to produce by the constructive Computer Aided Design (CAD) techniques and possesses all the specificity of metal foam. The physical model used for the present study is shown in Figure 1. To save computing time, a three-dimensional aluminum foam (20 mm × 20 mm × 10 mm) whose periodic cell size is 2.5 mm was chosen as the computational domain.

The composite material was heated from the left wall through a constant temperature (333.15 K) while the other walls were maintained adiabatic. The temperatures of the nanoPCMs and the aluminum foam were initially assumed to be 293.15 K. The initial velocity of the nanoPCM was zero and maintained no slip at the walls. The initial pressure was at atmospheric pressure. The thermo-physical properties of the different materials are represented in Table 1.

The heat transfer of composite PCM was very complicated during the phase change process including convective heat transfer between metal foam and liquid PCM, heat conduction between metal foam and solid PCM, natural convection of liquid PCM, etc. Hence the numerical simulation was carried out based on some assumptions:

(1) The Al_2O_3 nanoparticles were homogeneously distributed in the PCM.
(2) The melting of nanoPCM was Newtonian and incompressible, and its flow was three dimensional and unsteady.

Table 1. Thermal properties of paraffin, aluminum and Al_2O_3

Property	Material		
	Paraffin wax	Al_2O_3	Aluminum
Melting point (°C)	53.7	NA[a]	NA[a]
Latent heat of fusion (kJ/kg)	232	NA[a]	NA[a]
Thermal conductivity (W/m·K)	0.22/0.24	36	160
Density (kg/m^3)	790/910	3600	2680
Specific heat (J/kg·K)	2150/2000	765	963
Kinematic viscosity (m^2/s)	3.10^{-6}	NA[a]	NA[a]
Thermal expansion coefficient (1/°C)	1.10^{-3}	NA[a]	NA[a]

[a]Not applicable due to no phase change for the material.

(3) The physical properties of the nanoPCM were temperature dependent.
(4) The melting of nanoPCM was controlled by the convection and conduction modes of heat transfer.
(5) Thermal radiation within composite PCM was neglected.

2.1. *Governing equations*

The governing equations can be written as follow:

(1) Energy equation of heat transfer

The equation for the heat transfer of solid and liquid regions within nanoPCM is

$$\rho_{nf} C_{p_{nf}} \frac{\partial T_{nf}}{\partial t} + \rho_{nf} C_{p_{nf}} \vec{u} \cdot \vec{\nabla} T_{nf} = -\vec{\nabla} \cdot (-k_{nf} \vec{\nabla} T_{nf}) - \rho_{nf} L_f \frac{\partial B}{\partial t} \tag{1}$$

Equation for the heat transfer of metal foam:

$$\rho_s C_{p_s} \frac{\partial T_s}{\partial t} = -\vec{\nabla} \cdot (-k_s \vec{\nabla} T_s) \tag{2}$$

Equations (3) and (4) show the temperature and heat at the interface between nanoPCM and Aluminum foam respectively:

$$T_{nf} = T_s \tag{3}$$

$$k_{nf} \frac{\partial T_{nf}}{\partial \vec{n}} = k_s \frac{\partial T_s}{\partial \vec{n}} \tag{4}$$

where the subscript s and nf stand for the aluminum foam and the nanoPCM, respectively. Cp is the specific heat capacity; k is the thermal conductivity and ρ is the density.

(2) Equations of fluid dynamics:

Continuity equation:

$$\overline{\overline{\nabla}} \cdot \vec{u} = 0 \tag{5}$$

Momentum equation:

$$\rho_{nf} \frac{\partial \vec{u}}{\partial t} + \rho_{nf} \vec{u} \cdot (\overline{\overline{\nabla}} \vec{u}) - \mu_{nf} \vec{\nabla}^2 \vec{u} = -\vec{\nabla} P + \vec{F}_b + \vec{F}_a \tag{6}$$

where ρ_{nf} and μ_{nf} are the density and viscosity of nanoPCM, respectively. The force $\vec{F}_b$ is a buoyancy force can be given by the Boussinesq approximation:

$$\vec{F}_b = \rho_{nf} \vec{g} \beta (T_{nf} - T_m) \tag{7}$$

And the force $\vec{F}_a$ is an additional source to damp the velocity.

$$\vec{F}_a = -A(T) \cdot \vec{u} \tag{8}$$

With the function $A(T)$ inspired from the Carman–Koseny relation for porous medium [40]

$$A(T) = \frac{C(1-B(T))^2}{(q+B^3(T))} \tag{9}$$

where q is typically a small number so as to make (9) effective, even when the liquid fraction $B(T)$ is zero. The constant value of q was fixed at 10^{-3}. C defines the mushy zone constant and its value is subject to the morphology of the PCM. The mushy zone constant describes how steeply the velocity is totally reduced to zero when the PCM becomes completely solid. In this research, C is taken as a constant value 10^6 [23]. This value is chosen arbitrary high due to the high viscosity of solid PCM.

The function $B(T)$ given by (10) is defined as the liquid fraction. It was updated to account for the change in specific heat between the solid and the liquid phase of the PCM. The liquid fraction function B is defined as a function of temperature [28].

$$B(T) = \left\{ \begin{array}{ll} 0 & T < (T_m - \Delta T_m) \\ (T - T_m + \Delta T_m)/(2\Delta T_m), & (T_m - \Delta T_m) \leq T < (T_m + \Delta T_m) \\ 1 & T > (T_m + \Delta T_m) \end{array} \right\} \tag{10}$$

where, T_m is the melting temperature and ΔT_m is introduced to make the calculation easier.

The choice of the temperature transition range ΔT_m requires careful consideration. The sharp gradients of the modified heat capacity may lead to convergence issues if ΔT_m is small and the mesh resolution at the interface does not cover the imposed range. A small ΔT_m means greater accuracy coming with greater computational effort. The choice of the optimal value of this parameter ΔT_m has been validated against previous experimental results from literature in Section 3.

The liquid fraction of the PCM is used to model the modifications of the thermo-physical properties that appear during the phase transition.

2.2. *Thermo physical properties relations in the nanoPCM*

Transport of nanoparticles and their rejection by the advancing liquid–solid interface are ignored and it was assumed that the Al_2O_3 nanoparticles are homogenously distributed during the melting process. The thermal properties of such nanoPCM for varying volume fractions need to be properly calculated. The following formula relates the mass fraction ϕ_{wt} of alumina and its volume fraction ϕ:

$$\phi = \frac{\phi_{wt}\rho_{\mathrm{PCM}}}{\phi_{wt}\rho_{\mathrm{PCM}} + (1-\phi_{wt})\rho_{\mathrm{Al_2O_3}}} \tag{11}$$

where ρ_{PCM} and $\rho_{\mathrm{Al_2O_3}}$ are the density of PCM and the density of alumina nanoparticles, respectively.

The thermo physical properties such as density, specific heat, latent heat, thermal expansion coefficient are obtained with following equations similar to the procedure reported in [26]:

$$\rho_{nf} = (1-\phi)\rho_{\mathrm{PCM}} + \phi\rho_{\mathrm{Al_2O_3}} \tag{12}$$

The density of PCM can be written as:

$$\rho_{\mathrm{PCM}}(T) = \rho_{\mathrm{solid}} + (\rho_{\mathrm{liquid}} - \rho_{\mathrm{solid}})B(T) \tag{13}$$

where ρ_{liquid} and ρ_{solid} describe the density of the PCM at its liquid and solid phase respectively.

The modified heat capacity of the nanoPCM can be written as [41]:

$$Cp_{nf} = (1-\phi)Cp_{\mathrm{PCM}} + \phi Cp_{\mathrm{Al_2O_3}} \tag{14}$$

where Cp_{PCM} and $Cp_{\mathrm{Al_2O_3}}$ are the heat capacity of the PCM and the alumina nanoparticles, respectively.

The heat capacity of PCM is written as [42]:

$$Cp_{\mathrm{PCM}}(T) = Cp_{\mathrm{solid}} + (Cp_{\mathrm{liquid}} - Cp_{\mathrm{solid}})B(T) + L_f D(T) \tag{15}$$

where Cp_{solid} and Cp_{liquid} are the heat capacity of the PCM at its solid and liquid phases, respectively. $D(T)$ is defined as follows:

$$D(T) = e^{\left(\frac{-T_{nf}(T_{nf}-T_m)^2}{\Delta T_m{}^2} \Big/ \sqrt{\pi \cdot \Delta T_m{}^2}\right)} \tag{16}$$

With commercial codes, or fixed-mesh simulations, the codes do not appreciate discontinuities (discontinuities that would occur if a pure Dirac delta function was used to describe a phase change occurring at a specific temperature, rather only over a temperature range), then the energy impact of the phase change is stretched over a temperature range, eliminating discontinuities.

When the PCM starts to melt, it absorbs the latent heat (L_{f}) which can be representing as a change in its specific heat during the phase transition period.

The effective dynamic viscosity of the nanoPCM is evaluated by the Krieger–Dougherty model for nanoparticles [24].

$$\mu_{nf} = \frac{\mu_{\mathrm{PCM}}}{(1-\phi)^{2.5}} \tag{17}$$

The effective thermal conductivity of the nanoPCM is evaluated using a Maxwell–Garnett type effective medium theory (EMT) considering the role of thermal boundary resistance between the Al_2O_3 and surrounding PCM matrix. This model has proven to predict the thermal conductivity enhancement of nanoPCM with reasonable accuracy [23, 24]. Accordingly, the effective thermal conductivity of the colloid is the sum of thermal conductivity due to the Brownian motion of nanoparticle and stagnant thermal conductivity:

$$k_{nf} = k_d + k_0 \tag{18}$$

where k_0 is the stagnant thermal conductivity given by:

$$k_0 = k_{\mathrm{PCM}} \frac{k_{\mathrm{Al_2O_3}} + 2k_{\mathrm{PCM}} - 2\phi(k_{\mathrm{PCM}} - k_{\mathrm{Al_2O_3}})}{k_{\mathrm{Al_2O_3}} + 2k_{\mathrm{PCM}} + \phi(k_{\mathrm{PCM}} - k_{\mathrm{Al_2O_3}})} \tag{19}$$

The k_d accounts for the Brownian motion of the nanoparticles, which causes the temperature dependence of the thermal conductivity.

$$k_d = 5 \times 10^4 \beta_k \xi \phi (\rho Cp)_{\mathrm{PCM}} \sqrt{\frac{B_0 T}{\rho_n d_p}} f(T, \phi) \tag{20}$$

where

$$f(T,\phi) = (2.8217 \times 10^{-2}\phi + 3.917 \times 10^{-3}) \frac{T}{T_{ref}} + (-3.0669 \times 10^{-2}\phi - 3.91123 \times 10^{-3}) \tag{21}$$

B_0 is Boltzmann constant, 1.381×10^{-23} J/K and d_{p} is the diameter of nanoparticles. The value of $\beta_k = 8.4407(100\phi)^{-1.07304}$.

The value of correction factor ξ, in the Brownian motion term is defined as the same as for liquid fraction, $B(T)$ in (10).

3. Numerical model

The thermal model mentioned in Section 2 was solved numerically by the commercial software Comsol Multiphysics based on the finite element method. The physical properties of

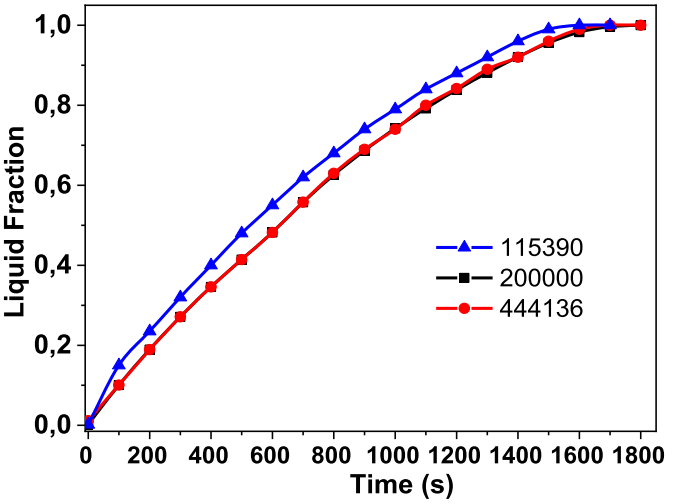

Figure 2. Mesh independence analysis.

nanoPCM/metal foam were defined according to temperature, which determines the phase (liquid, mushy, or solid), the nanoparticles concentration (ϕ), the porosity of metal foam (ε).The numerical simulation was carried out according to the following steps: Discretization of the considered domain (size, element and type), defining the appropriate time step as well as the relative and absolute tolerances and using the appropriate solver techniques. In order to find the appropriate solution, a mesh dependence study was performed carefully for the current investigation. A triangular meshing with a regular refinement method was used for the global mesh at the macro scale geometry of the composite material. The structured grids were built within the aluminum foam and the pore space impregnated with nanoPCM (Paraffin wax/Al_2O_3). The mesh sensitivity test was carried out adopting three different level meshes with 115390, 200000 and 444136 cells, as presented in Figure 2. By comparing the results of the three meshes, we can see that the differences of liquid fraction for meshes with 200000 and 444136 cells are less than 2%, and the three meshes have almost the same prediction results. Considering the accuracy and the time of the numerical calculation, 200000 cells can ensure the mesh independence.

An absolute tolerance of 0.00001 and a relative tolerance of 0.001 were applied. The time step ranged between 0.01s and 100 s.

For validation, the calculations from the present simulation model were compared with the experimental results achieved by Li *et al.* [38] with the same material properties and similar boundary conditions as plotted in Figure 3. The numerical results of the temperature variation for pure PCM and composite PCM with a porosity (ε) of 0.9 and a pore density (ω) of 10PPI are in good agreement with the experimental study of Li *et al.* [38].

In addition, the effect of the melting temperature range on the melting interface position was studied for 2 K and 5 K melting temperature ranges. The temperature variation for the 2 K melting temperature ranges present best fit to the reported results from Li *et al.* [38]. Such a comparative analysis could be a rigorous test for the coherence of our model, which allows to use it later.

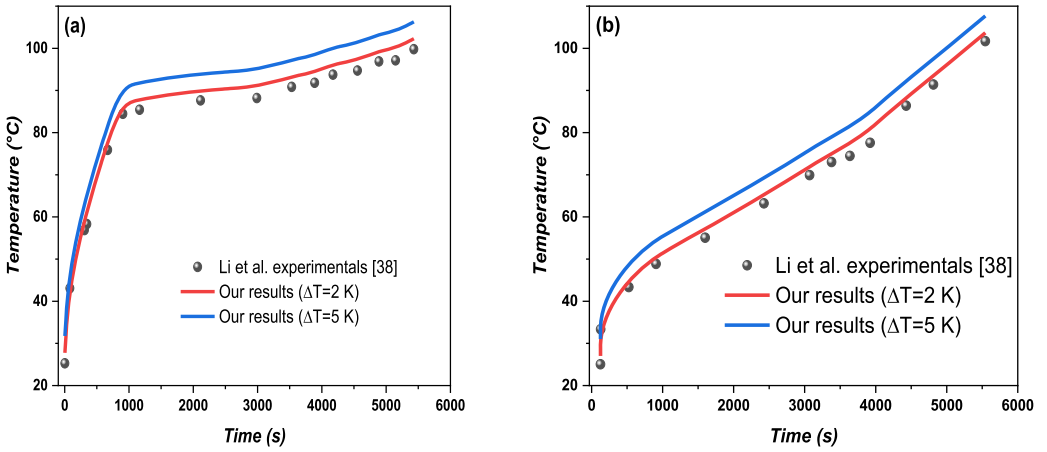

Figure 3. Validation of Temperature variation with experimental data of Li *et al.* [38]. (a) Pure PCM and (b) PCM/metal foam ($\varepsilon = 0.9$; $\omega = 10$ PPI).

4. Results and discussion

4.1. *Melting process*

The rate of melting is considered as an important factor in many engineering applications, such as the latent heat thermal energy storage systems. We investigated the effect of Al_2O_3 nanoparticles and aluminum foam on the performance of the latent heat storage unit. Figure 4 shows the variation of the liquid fraction for composite PCMs with different parameters during the melting process. Figure 4a shows the liquid fraction plotted against time for paraffin wax and paraffin wax with alumina particles at different volume fractions. It took 6600 s for pure PCM to achieve the melting process, 6100 s for $\phi = 1\%$, 5700 s for $\phi = 3\%$, and 6500 s for $\phi = 5\%$. Additionally, it is observed that the melting rate of 3% Al_2O_3 is faster and that of 5% Al_2O_3 is slower than that of simple paraffin wax. Dispersing nanoparticles at $\phi = 1\%$ shows a gentle impact on melting time (7.57% less), while the total melting time was shortened by nearly 13.64% for $\phi = 3\%$. The melting time decreased with the increase in volume fractions of nanoparticles by 3% and 1%. Whereas, it is observed that the melting rate of 5% Al_2O_3 is approximately the same as that of the pure PCM due to the increase in viscosity that weakened the buoyancy effect. Normally, the conductivity and the viscosity of PCM increase with the addition of nanoparticles. At high volumetric fractions of nanoparticles, the negative effect of the increase in viscosity may become homologous to the positive effect of conductivity enhancement of nanoPCM on the heat transfer and therefore on the melting process. Figure 4b evaluates composite PCMs (Paraffin wax/metal foam) with different porosities ($\varepsilon = 0.9$; 0.95; 0.98). It compares the pure PCM with the PCM/metal foam in terms of average liquid fraction. The difference between the pure paraffin and the PCM/metal foam is evident; in fact the presence of the foam improves significantly the heat transfer and, thus, the melting rate. For example the time of melting for the PCM with metal foam at a porosity of 0.98 is 4500 s, while for the pure Paraffin the melting time is 6600 s. Therefore higher values of porosity decrease the rate of melting; in fact at a porosity of 0.9, the melting time is 1800 s. As for the liquid fraction of the composite (nanoPCM/metal foam) shown in Figure 4c, the melting times of the nanoPCM embedded in aluminum foam were 1600 s and 3400 s at porosities of 0.9 and 0.98, respectively. The melting times for all composite PCMs with different parameters are shown in Figure 5. It is observed that the melting time of composite PCM with the same volume fractions increased with the increase in porosity. In addition, the melting time

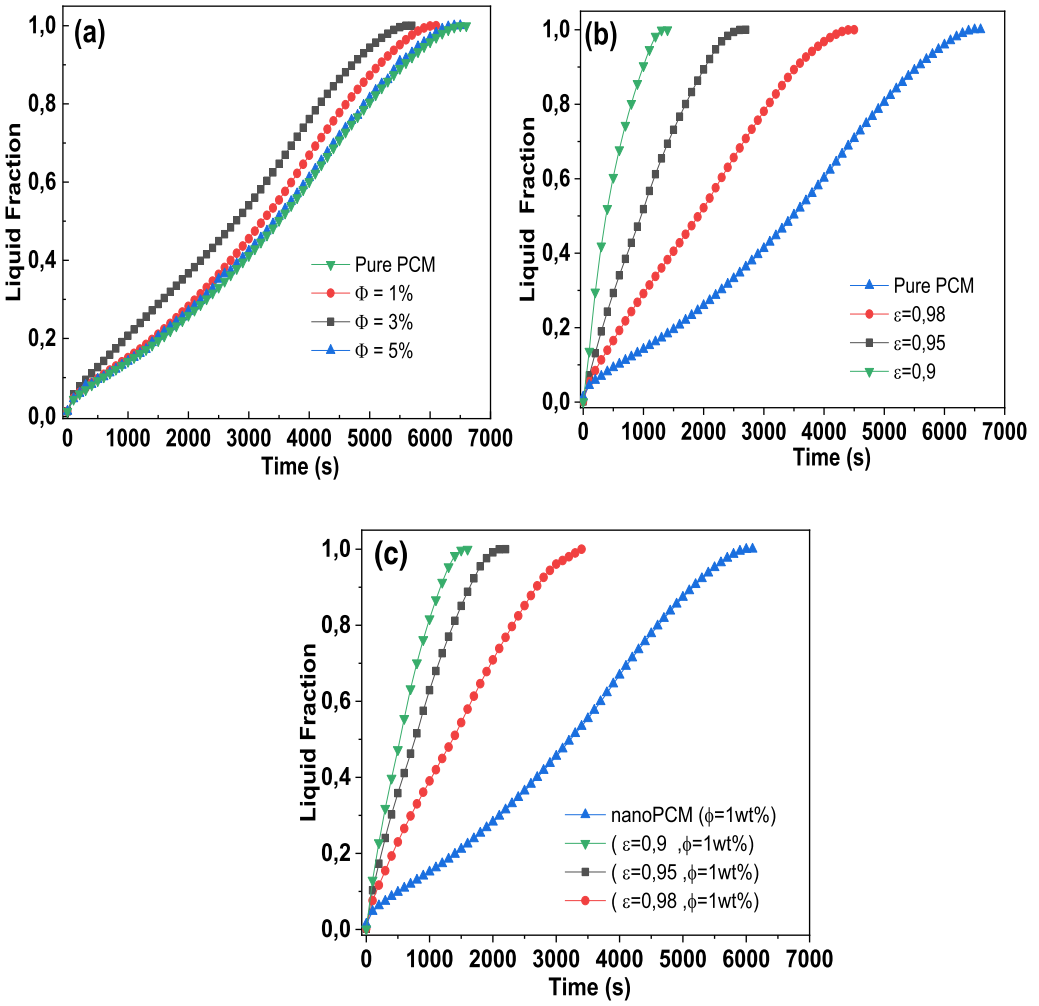

Figure 4. The liquid fraction with melting time for composite PCMs: (a) Paraffin wax/Al_2O_3 at different volume fractions, (b) Paraffin wax/metal foam at different porosities, (c) NanoPCM (1% volume fraction)/metal foam at different porosities.

for composite PCMs with 2% Al_2O_3 is higher than that of composite PCMs with 1% Al_2O_3 at the same porosity. This reveals that the volume fractions and porosity have a significant influence on the melting time of composite PCM. Concurrently, it is established that the addition of aluminum foam and alumina nanoparticles to paraffin wax increased the melting rate of composite PCM.

Figure 6 presents the melting rate of different composite PCMs for two selected times (1000 s and 3000 s) during the phase change process. In addition, it compares the evolution of liquid fraction for pure PCM and nanoPCM ($\phi = 1\%$) with and without aluminum foam ($\varepsilon = 0.98$).

The region of the liquid fraction set two limits: 0 for solid phase with blue color and 1 for the liquid phase with red color. Thevalues between 0 and 1 indicate the mushy zone (mixture of solid and liquid phases). At 1000 s, adding nanoparticles slightly enhanced the melting process from 13.1% for pure PCM to 16.5% for nanoPCM; whereas the addition of metal foam has critical influence on the melting process from 29.1% for pure PCM to 39% for nanoPCM. The incorporation of the metal foam can enhance the melt fraction due to the increase in the heat

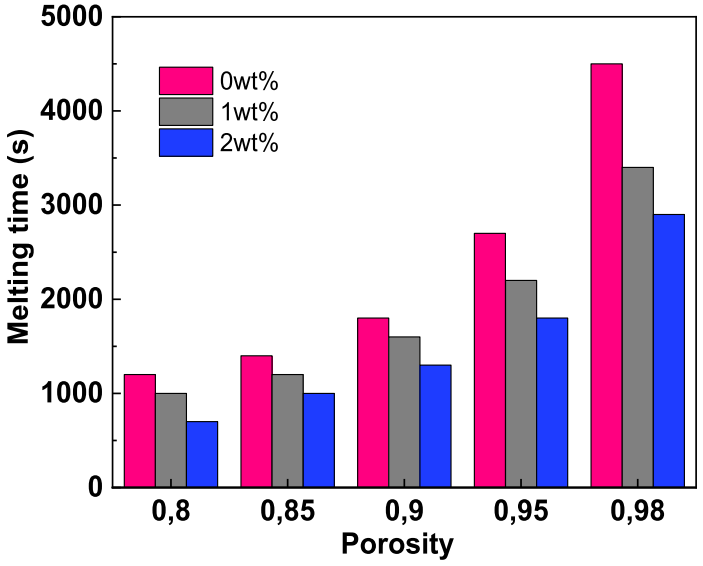

Figure 5. The variation of melting time for Composite PCMs (nanoPCM/metal foam) at different porosities and volume fractions.

transfer surface and heat diffusion within the porous media. Compared with the PCM/metal foam results, the melting process of the nanoPCM/metal foam significantly improved (from 78% to 96% at 3000 s) due to the higher thermal conductivity of the nanoPCM in metal foam. It is well established that the Al_2O_3 nanoparticles inside the aluminum foam can be either deposited on the pore surface (i.e. non-plugging pathway) or structured in particle bridge across the pore (i.e., plugging pathway) to improve the effective thermal conductivity further. The shape of the PCM melting front with aluminum foam tends to be straighter than that without metal foam.

Figure 7 shows the melting process of the nanoPCM inside aluminum foam ($\varepsilon = 0.95$) at pore scale. The red color denotes the liquid-phase region, the blue color denotes the solid-phase region and the other color indicates the mushy region. During the melting process, the liquid-phase zone and the mushy zone increased progressively, while the solid-phase zone decreased. The figure also reveals that the nanoPCM neighboring the foam metal frame is the first to reach the phase change temperature and melt. At the beginning of the melting process, the nanoPCM at the heat source surface melted first, followed by the nanoPCM around the aluminum foam frame and then gradually moved to the center of the pores. The heat was transmitted to all the structure due to the high thermal conductivity of metal foam, inducing the melting of the paraffin wax surrounding the metal. Therefore, the solid-liquid interface of the nanoPCM extends from the boundary of the paraffin wax and foam metal frame to the center of pore, making the solid nanoPCM surrounded by the melting one.

4.2. *Temperature distribution*

Figure 8 shows the variation of the temperature for Composite PCMs with different parameters during the melting process. It can be seen from these curves that the evolution of temperature as a function of time of pure paraffin and of composite materials are divided into three steps (pre-melting, melting and post-melting). During the first step of the melting process, when $t < 1200$ s for pure PCM and nanoPCM and $t < 500$ s for the composite material, the temperature of the pure PCM and that of the composite increased by absorbing a large sensible of PCM and latent heat.

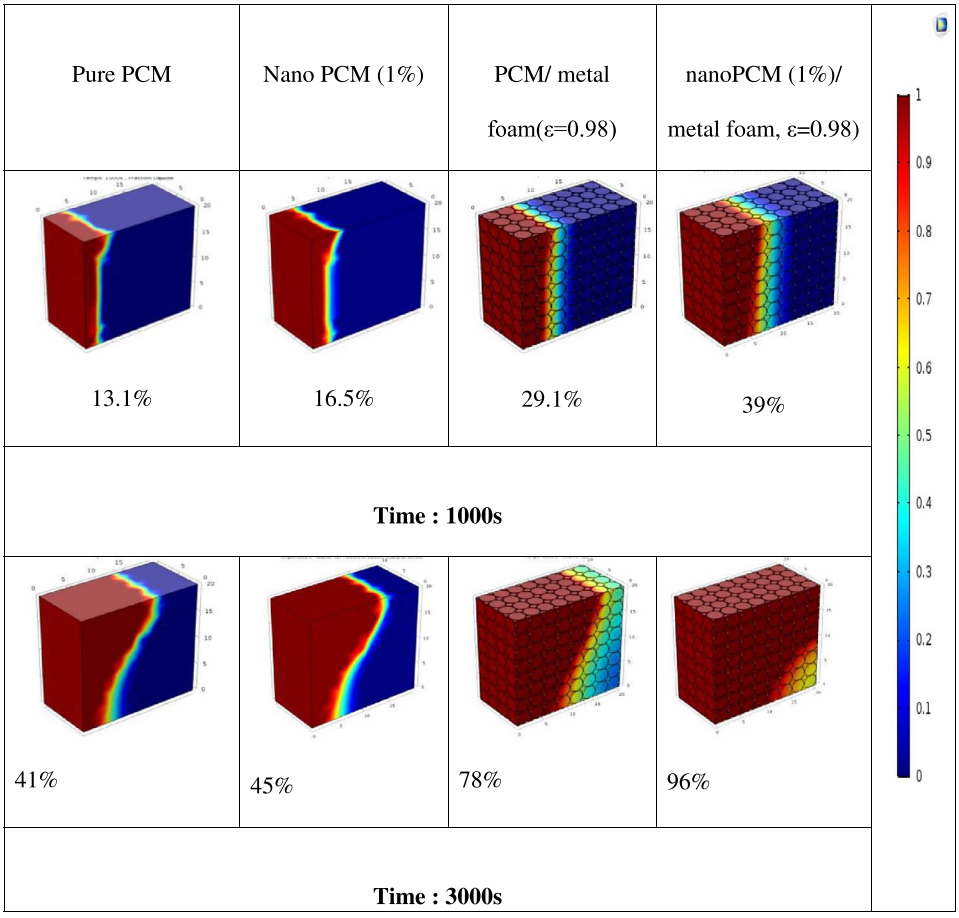

Figure 6. The evolution of melting process for pure PCM, PCM/metal foam and nanoPCM within and without metal foam.

Then during the melting process, two factors dominated the phase change: the heat conduction and the natural convection of the molten PCM. For the pure PCM, the Paraffin absorbed the latent melting heat at the solid/liquid interface dominated by natural convection, thereby increasing the temperature of the pure paraffin in a flattened manner. However, the temperature of the composite material increased by the combined effects of heat diffusion, natural convection, and the absorption of latent heat at the front of displacement. When the melting process is finished, the explicit heat exerted its role again and the temperatures of the pure PCM and the composite continued to increase linearly. Figure 9 displays the effect of porosity on the temperature response of the metal foam filled with nanoPCM. In general, a lower porosity ensures a higher temperature. This result occurs because the smaller porosity, the more the PCM in the sample induces higher thermal diffusivity and larger latent heat capacity. The fraction of metal foam increased with the decrease of the porosity of the PCM composite. The increased fraction of metal means a higher effective thermal conductivity, which helps to conduct heat away rapidly. The decrease in the amount of PCM in the system, makes the sensible heat greater than the latent heat. The average temperature evolution of different specimens along the x-direction at 1000th second is shown in Figure 10. The green curve represents the temperature distribution of the pure PCM. The other colors denote the temperature distribution of the Composite PCMs

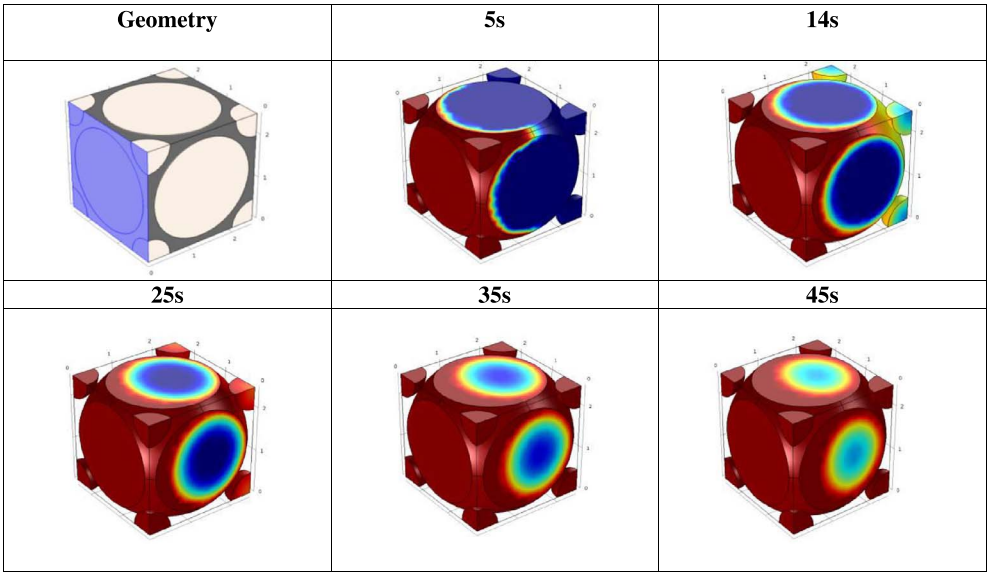

Figure 7. Variation of liquid fraction of PCM composite ($\phi = 1\%$, $\varepsilon = 0.95$) at pore scale.

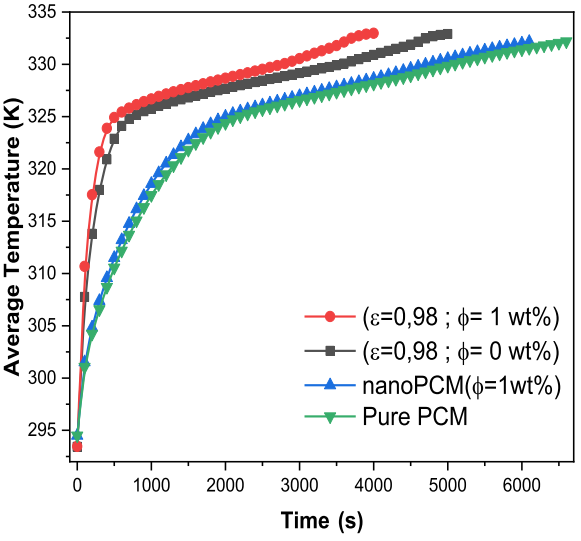

Figure 8. Average temperature evolution during the time for different composite PCMs.

(nanoPCM/aluminum foam) with different porosities. This figure illustrates that the temperature variation along the x direction of the Composite PCMs was more homogeneous than that of the pure paraffin. Concurrently, the distribution of the material with small porosity is more uniform.

Figure 11 shows the temperature difference between the metal foam taken at 5 locations (T1, T3, T5, T7, and T9) and the PCM at 5 different locations (T2, T4, T6, T8, T10) within the composite PCM at a porosity 0.9. The difference of temperatures increased at the start of melting and then decreased, which proves the feasibility of the local thermal non-equilibrium within composite PCM during the melting process. At the beginning of the melting process,

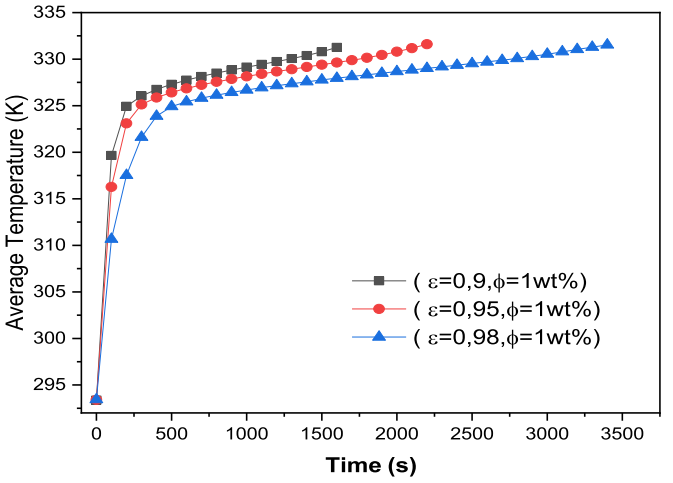

Figure 9. Average temperature evolution during the time for composite PCM (nanoPCM/aluminum foam at different porosity).

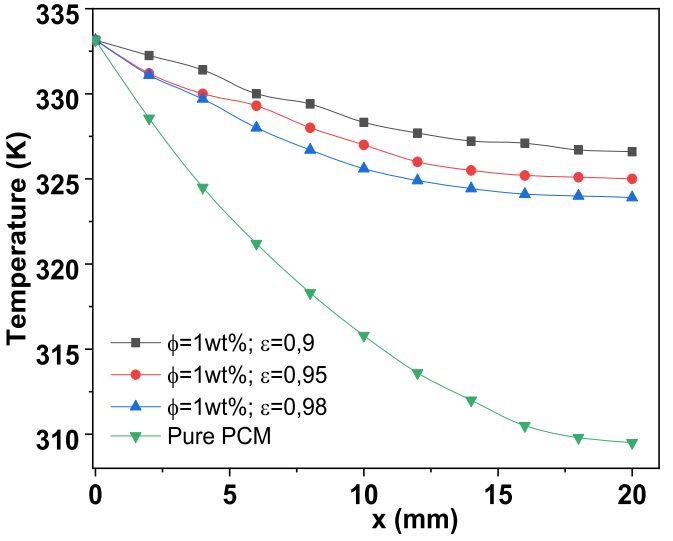

Figure 10. The variation of temperature for Pure Paraffin and composite PCMs (nanoPCM/metal foam) with different porosities along of x-direction at 1000 s.

the temperature difference of the location near the heated wall (T1/T2 and T3/T4) was higher than that of the location far from the heated wall (T5/T6 and T7/T8). The temperature of the aluminum ligament was initially greater than that of the PCM or nanoPCM. This is due to the high thermal conductivity of aluminum foam which allows the rapid transfer of the heat and the abrupt increase in the temperature of the metal, while that of the PCM remained relatively slow. After some time, the temperature difference decreased due to the heat conduction between PCM and metal foam. Upon phase change, the temperature differences are relatively stable because paraffin consumed heat and changed state, which results from the combined effect of heat diffusion and natural convection.

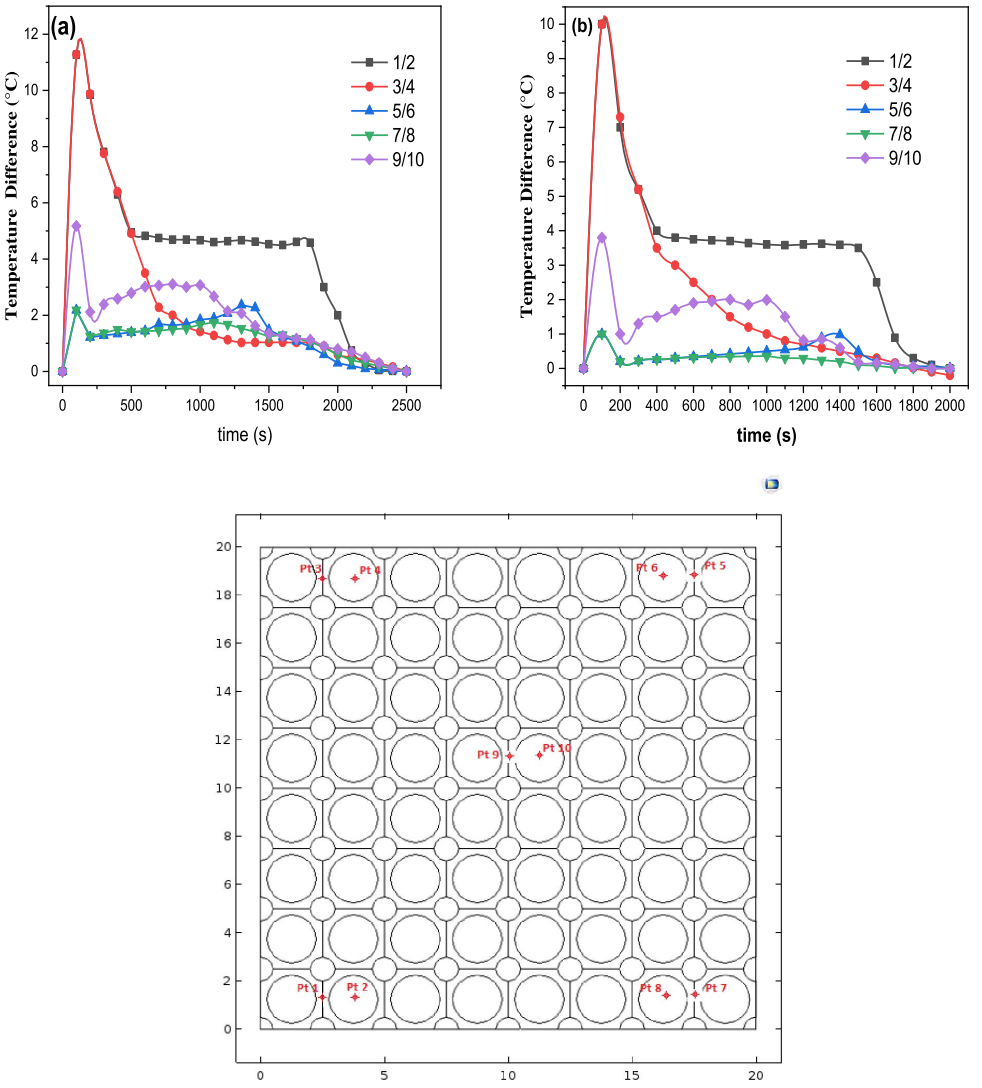

Figure 11. Temperature difference between aluminum skeleton and paraffin at different locations for composite PCMs: (a) paraffin wax/metal foam ($\varepsilon = 0.9$); (b) NanoPCM ($\phi = 1\%$)/metal foam ($\varepsilon = 0.9$).

Thanks to the natural convection improvement at the liquid phase for paraffin, the temperature difference decreased to 0 °C, ultimately advancing local thermal equilibrium between aluminum ligament and PCM. The incorporation of 1% Al_2O_3 into the composite (Paraffin/metal foam) decreased the temperature difference between the ligament and PCM due to the high thermal conductivity of alumina and accelerated the melting process.

4.3. *Velocity variations*

The velocity field of nanoPCM ($\phi = 1\%$) embedded in Aluminum foam ($\varepsilon = 0.95$) at different times is presented in Figure 12. It is noted that the range of velocity distribution gradually increased as the melting progressed, which reveals that the natural convection is strengthened. It is also

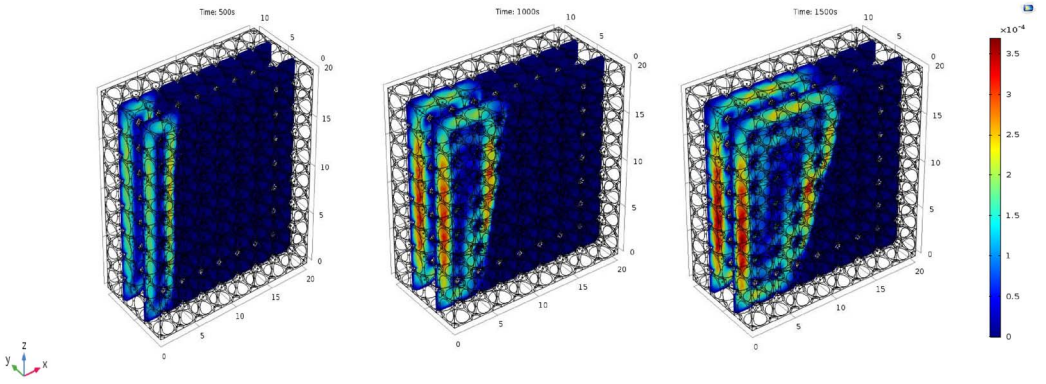

Figure 12. The distribution of velocity field of PCMs composite (ϕ = 1%, ε = 0.95) with different times.

observed that the velocity magnitude near the heated wall and in the melting front is considerably higher than the other parts. The natural convection is greatly accentuated at the left top domain of the composite PCM. Figure 13 shows the velocity arrows of the Composite PCM in y = 3 mm section at 1000 s. The velocity of the liquid nanoPCM proximate to the heated wall emerges to the top area, while that close to the melting front flows down, returning into a circle flow to the heated wall. The flow circulation of the liquid nanoPCM is quite distinct, due to the buoyancy effect resulting from the temperature difference. Furthermore, it is observed that the local circulation concentrates around the aluminum ligament. This phenomenon proves the weakness of the heat conduction improvement through the aluminum foam and strengthens the heat transfer between the nanoPCM and the metal within the composite PCM by the natural convection.

4.4. *Effective thermal conductivity*

Based on different parameters, the effective thermal conductivity was calculated and represented in Figure 14. It is noted that the thermal conductivity of the composite PCMs (nanoPCM/aluminum foam) at the same volume fractions of nanoparticles decreased as the porosity increased. Also, the effective thermal conductivity for the composite PCMs with 1% of Al_2O_3 is shorter than that of the composite PCMs with 2% of Al_2O_3 when the porosity of the composite PCMs is the same. The thermal conductivity of pure paraffin is 0.22 W/(m·K).

The high porosities are associated with a low volume of metal which resulted in a decrease in the conductive paths for heat flow. Although the metal occupies a very small fraction of the volume in the composite, the effective thermal conductivity increased by 38 times and 8.5 times more than that of the pure paraffin for the composite aluminum foam/paraffin at porosities of 0.9 and 0.98, respectively.

5. Conclusion

In this paper, we have investigated the thermal behavior of composite PCMs with different parameters at pore scale. A Direct Numerical Simulation (DNS) was carried out to study the melting process of paraffin wax enhanced with alumina nanoparticles (i.e. nanoPCM) embedded in aluminum foam with regular structure.

The results showed that both alumina nanoparticles and metal foam increased the effective thermal conductivity of the composite PCMs and accelerated the melting process. The addition

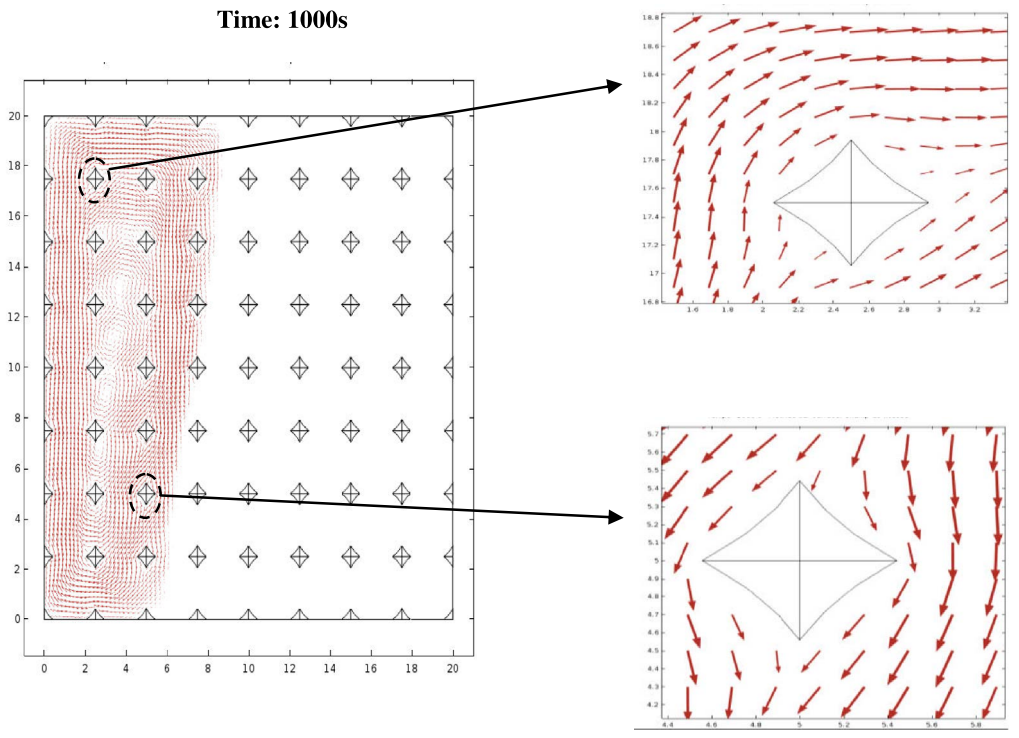

Figure 13. Velocity map of nanoPCM ($\phi = 1\%$) within composite PCM ($\varepsilon = 0.95$) at $t = 1000$ s.

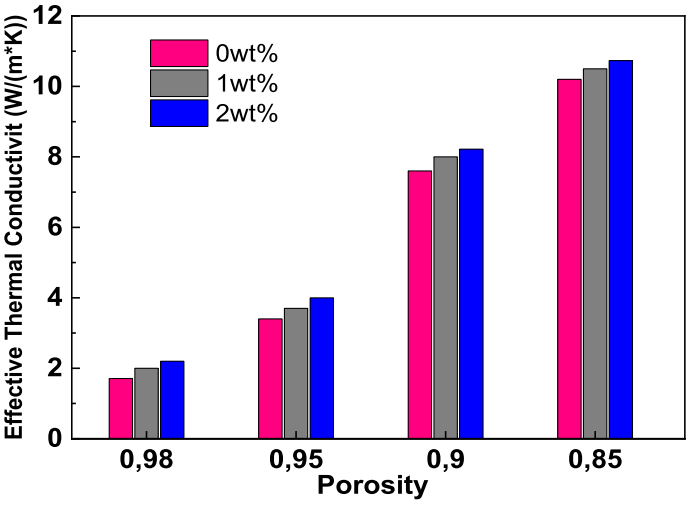

Figure 14. The effective thermal conductivity of composite PCMs (nanoPCM/metal foam) at different porosities and volume fractions.

of aluminum foam has more influence than the nanoparticles on the thermal behavior. The important Temperature difference between metal foam and PCM proves the feasibility to use the non-local thermal equilibrium. Additionally, the incorporation of 1% Al_2O_3 into the composite (Paraffin/metal foam) decreased the temperature difference between the aluminum ligament

and PCM. The addition of nanoparticles and metal foam to PCMs improved their thermal behavior, which makes them more suitable for thermal energy storage applications.

References

[1] S. Gong, Z. H. Zhu, Z. Li, "Electron tunnelling and hopping effects on the temperature coefficient of resistance of carbon nanotube/polymer nanocomposites", *Phys. Chem. Chem. Phys.* **19** (2017), p. 5113-5120.

[2] M. Iten, S. Liu, "A work procedure of utilising PCMs as thermal storage systems based on air-TES systems", *Energy Convers. Manag.* (2014), p. 608-627.

[3] H. Akeiber, P. Nejat *et al.*, "A review on phase change material (PCM) for sustainable passive cooling in building envelopes", *Renewable and Sustainable Energy Reviews* **60** (2016), p. 1470 - 1497.

[4] M. M. Kenisarin, K. M. Kenisarina, "Form-stable phase change materials for thermal energy storage", *Renew. Sustain. Energy Rev.* **16** (2012), p. 1999-2040.

[5] Y. Lin, G. Alva, G. Fang, "Review on thermal performances and applications of thermal energy storage systems with inorganic phase change materials", *Energy* (2018), p. 685-708.

[6] Z. Khan, Z. A. Khan, "An experimental investigation of discharge/solidification cycle of paraffin in novel shell and tube with longitudinal fins based latent heat storage system", *Energy Convers. Manag.* **154** (2017), p. 157-167.

[7] H. Zheng, C. Wang, Q. Liu, Z. Tian, X. Fan, "Thermal performance of copper foam/paraffin composite phase change material", *Energy Convers. Manag.* **157** (2018), p. 372-381.

[8] M. Jafari, A. Rahimi, P. Shokrolahi, A. E. Langroudi, "Synthesis of antistatic hybrid nanocomposite coatings using surface modified indium tin oxide (ITO) nanoparticles", *J. Coatings Technol. Res.* (2014), p. 587-593.

[9] C. Liang, X. Lingling, S. Hongbo, Z. Zhibin, "Microencapsulation of butyl stearate as a phase change material by interfacial polycondensation in a polyurea system", *Energy Convers. Manag.* (2009), p. 723-729.

[10] S. Ebadi, S. H. Tasnim, A. A. Aliabadi, S. Mahmud, "Melting of nano-PCM inside a cylindrical thermal energy storage system: numerical study with experimental verification", *Energy Convers. Manag.* (2018), p. 241-259.

[11] R. N. Das, F. D. Egitto, B. Wilson, M. D. Poliks, V. R. Markovich, "Polymer nanocomposites, printable and flexible technology for electronic packaging", *Proc. - 2009 Int. Symp. Microelectron. IMAPS 2009* (2009), p. 1.

[12] R. Yuksel, N. Uysal, A. Aydinli, H. E. Unalan, "Paper based, expanded graphite/polypyrrole nanocomposite supercapacitors free from binders and current collectors", *J. Electrochem. Soc.* **165** (2018), p. A283-A290.

[13] I. Rahim, M. Shah, M. Iqbal, F. Wahab, A. Khan, S. H. Khan, "Fabrication and electrical characterizations of graphene nanocomposite thin film based heterojunction diode", *Phys. B Condens. Matter.* (2017), p. 97-103.

[14] S. Shrivastava, N. Jadon, R. Jain, "Next-generation polymer nanocomposite-based electrochemical sensors and biosensors: a review", *TrAC - Trends Anal. Chem.* **82** (2016), p. 55-67.

[15] M. Jafari, A. Rahimi, P. Shokrolahi, A. E. Langroudi, "Synthesis of antistatic hybrid nanocomposite coatings using surface modified indium tin oxide (ITO) nanoparticles", *J. Coatings Technol. Res.* (2014), p. 587-593.

[16] A. J. Webb, M. Szablewski, D. Bloor, D. Atkinson, A. Graham, P. Laughlin, D. Lussey, "A multi-component nanocomposite screen-printed ink with non-linear touch sensitive electrical conductivity", *Nanotechnology* (2013), article no. 23535342.

[17] M. T. Chaichan, S. H. Kamel, A.-M. N. M. Al-Ajeely, "Thermal conductivity enhancement by using nano-material in phase change material for latent heat thermal energy storage systems", *Saussurea* (2015), p. 48-55.

[18] K. Akamatsu, M. Ogawa, R. Katayama, K. Yonemura, S. ichi Nakao, "A facile microencapsulation of phase change materials within silicone-based shells by using glass capillary devices", *Colloids Surfaces A Physicochem. Eng. Asp.* (2019), p. 297-303.

[19] S. Chowdhury, M. Olima, Y. Liu, M. Saha, J. Bergman, T. Robison, "Poly dimethylsiloxane/carbon nanofiber nanocomposites: fabrication and characterization of electrical and thermal properties", *Int. J. Smart Nano Mater.* **7** (2016), p. 236-247.

[20] B. Li, W. H. Zhong, "Review on polymer/graphite nanoplatelet nanocomposites", *J. Mater. Sci.* **46** (2011), p. 5595-5614.

[21] R. M. Mutiso, "Electrical percolation in metal nanowire networks for bulk polymer nanocomposites and transparent conductors, and resistive switching in metal/polymer nano-gap devices", ProQuest Diss. Theses, 2013.

[22] A. Karaipekli, A. Biçer, A. Sarı, V. V. Tyagi, "Thermal characteristics of expanded perlite/paraffin composite phase change material with enhanced thermal conductivity using carbon nanotubes", *Energy Convers. Manag.* **134** (2017), p. 373-381.

[23] F. Agyenim, N. Hewitt, P. Eames, M. Smyth, "A review of materials, heat transfer and phase change problem formulation for latent heat thermal energy storage systems (LHTESS)", *Renew. Sustain. Energy Rev.* (2010), p. 615-628.

[24] M. Li, "A nano-graphite/paraffin phase change material with high thermal conductivity", *Appl. Energy* **106** (2013), p. 25-30.

[25] Z. Ling, J. Chen, T. Xu, X. Fang, X. Gao, Z. Zhang, "Thermal conductivity of an organic phase change material/expanded graphite composite across the phase change temperature range and a novel thermal conductivity model", *Energy Convers. Manag.* **102** (2015), p. 202-208.

[26] M. Alimohammadi, Y. Aghli, E. S. Alavi, M. Sardarabadi, M. Passandideh-Fard, "Experimental investigation of the effects of using nano/phase change materials (NPCM) as coolant of electronic chipsets, under free and forced convection", *Appl. Therm. Eng.* **111** (2017), p. 271-279.

[27] S. Motahar, A. A. Alemrajabi, R. Khodabandeh, "Experimental study on solidification process of a phase change material containing TiO2 nanoparticles for thermal energy storage", *Energy Convers. Manag.* (2017), p. 162-170.

[28] K. Kant, A. Shukla, A. Sharma, P. Henry Biwole, "Heat transfer study of phase change materials with graphene nano particle for thermal energy storage", *Sol. Energy* **146** (2017), p. 453-463.

[29] A. V. Arasu, A. S. Mujumdar, "Numerical study on melting of paraffin wax with Al_2O_3 in a square enclosure", *Int. Commun. Heat Mass Transf.* (2012), p. 8-16.

[30] Y. Wang, X. Gao, P. Chen, Z. Huang, T. Xu, Y. Fang, Z. Zhang, "Preparation and thermal performance of paraffin/Nano-SiO_2 nanocomposite for passive thermal protection of electronic devices", *Appl. Therm. Eng.* **96** (2016), p. 699-707.

[31] A. H. N. Shirazi, F. Mohebbi, M. R. Azadi Kakavand, B. He, T. Rabczuk, "Paraffin nanocomposites for heat management of lithium-ion batteries: a computational investigation", *J. Nanomater.* (2016), article no. 2131946.

[32] M. Martinelli, F. Bentivoglio, A. Caron-Soupart, R. Couturier, J. F. Fourmigue, P. Marty, "Experimental study of a phase change thermal energy storage with copper foam", *Appl. Therm. Eng.* (2016), p. 247-261.

[33] S. T. Hong, D. R. Herling, "Open-cell aluminum foams filled with phase change materials as compact heat sinks", *Scr. Mater.* (2006), p. 887-890.

[34] X. Xiao, P. Zhang, M. Li, "Effective thermal conductivity of open-cell metal foams impregnated with pure paraffin for latent heat storage", *Int. J. Therm. Sci.* (2014), p. 94-105.

[35] W. Li, H. Wan, H. Lou, Y. Fu, F. Qin, G. He, "Enhanced thermal management with microencapsulated phase change material particles infiltrated in cellular metal foam", *Energy* (2017), p. 671-679.

[36] Z. Chen, D. Gao, J. Shi, "Experimental and numerical study on melting of phase change materials in metal foams at pore scale", *Int. J. Heat Mass Transf.* (2014), p. 646-655.

[37] Y. B. Tao, Y. You, Y. L. He, "Lattice Boltzmann simulation on phase change heat transfer in metal foams/paraffin composite phase change material", *Appl. Therm. Eng.* **93** (2016), p. 476-485.

[38] W. Q. Li, Z. G. Qu, Y. L. He, W. Q. Tao, "Experimental and numerical studies on melting phase change heat transfer in open-cell metallic foams filled with paraffin", *Appl. Therm. Eng.* **37** (2012), p. 1-9.

[39] R. Hossain, S. Mahmud, A. Dutta, I. Pop, "Energy storage system based on nanoparticle-enhanced phase change material inside porous medium", *Int. J. Therm. Sci.* (2015), p. 49-58.

[40] A. D. Brent, V. R. Voller, K. J. Reid, "Enthalpy-porosity technique for modeling convection-diffusion phase change: application to the melting of a pure metal", *Numer. Heat Transf.* **13** (1988), p. 297-318.

[41] N. S. Dhaidan, J. M. Khodadadi, T. A. Al-Hattab, S. M. Al-Mashat, "Experimental and numerical investigation of melting of NePCM inside an annular container under a constant heat flux including the effect of eccentricity", *Int. J. Heat Mass Transf.* **67** (2013), p. 455-468.

[42] P. H. Biwole, P. Eclache, F. Kuznik, "Phase-change materials to improve solar panel's performance", *Energy Build.* **62** (2013), p. 59-67.